FINAL REPORT

Project B-207

RESEARCH STUDY ON PANEL FLUTTER AERODYNAMICS

By

E. F. E. Zeydel

Contract NAS 8-20100

Prepared for
George C. Marshall Space Flight Center
National Aeronautics and Space Administration
Huntsville, Alabama

GEORGIA INSTITUTE OF TECHNOLOGY
Atlanta, Georgia

During the course of the program, the wind tunnel models and the boundary layer probe were fabricated. The wind tunnel tests were carried out at the 2 x 2 foot transonic research tunnel located at the NASA Ames Research Center, Moffett Field, California. The tunnel had a splitter plate which was designed to vary the boundary layer thickness over the surface of the plate. The wind tunnel models had a two dimensional, sinusoidally shaped surface and were mounted on the splitter plate. The boundary layer probe had the capability to traverse the boundary layer in two mutually perpendicular directions.

It was the purpose of the tests to measure the static pressure distribution on the surface of the models and within the boundary layer. A comparison with theoretical analysis could then be made.

Due to various circumstances only a cursory evaluation of experimental data and a few checks with theoretical predictions have been made during this program. This information indicates, however, that the experimental data is excellent and that good agreement with theoretical predictions can be expected. It is anticipated to conduct a more detailed evaluation of the data in the near future.

I. INTRODUCTION

In recent years much attention has been devoted to panel flutter instability, both theoretically and experimentally. The complexity of the phenomena has resulted in the necessity of developing separate design criteria for a variety of flow conditions and panel configurations. For the Saturn vehicle, panel configurations with very low aspect ratios are of specific interest and the region of low supersonic flow, where boundary layer effects are important, becomes critical.

In a previous program [1]* sponsored by the George C. Marshall Space Flight Center (Contract No. NAS8-11396), a new method was presented for predicting flutter boundaries for very low aspect ratio flat panels. The method is based on linearized, three dimensional potential flow theory and small deflection plate theory. In [1], the preliminary studies for an experimental investigation of the effects of a turbulent boundary layer on the pressure distribution on sinusoidal wavy walls are also given. These studies consist of a specification of model parameters and the design of a boundary layer probe.

This report is concerned with the research work performed as a continuation of the program mentioned above.

A more convenient method for solving the flutter equations for low aspect ratio panels is given. The method should considerably reduce computation time for obtaining flutter boundaries.

---

* Numbers in square brackets refer to items in the references.

GEORGIA INSTITUTE OF TECHNOLOGY
School of Aerospace Engineering
Atlanta, Georgia 30332

FINAL REPORT

Project B-207

RESEARCH STUDY ON PANEL FLUTTER AERODYNAMICS

by

E. F. E. ZEYDEL

Contract NAS 8-20100

Prepared for
GEORGE C. MARSHALL SPACE FLIGHT CENTER
NATIONAL AERONAUTICS AND SPACE ADMINISTRATION
Huntsville, Alabama

ABSTRACT

A new method for solving the flutter equations for low aspect ratio flat panels is presented. The method is an extension of the work given in [1].

Two dimensional sinusoidal wavy wall models were tested in the Mach number region $0.6 \leq M \leq 1.4$. The prime objective of these tests was to provide static pressure measurements on the surface of the models and within the turbulent boundary layer of variable thickness for comparison with theoretical analysis.

Only a cursory evaluation of experimental data is given.

PREFACE

This report covers theoretical and experimental investigations sponsored by the National Aeronautics and Space Administration, George C. Marshall Space Flight Center, Huntsville, Alabama, under Contract No. NAS 8-20100. The work was administered by Mr. R. G. Beranek of the Aeroballistics Laboratory.

The principal investigator of the program was Dr. E. F. E. Zeydel.

This report covers research work done during the period April 5, 1965 to November 4, 1966.

The author wishes to acknowledge the contributions of Mr. L. H. Knight and Mr. J. E. Sims for the design of the boundary layer probe and Mr. A. C. Bruce and Mr. N. R. Maddox for their contributions in the supporting analysis.

TABLE OF CONTENTS

LIST OF FIGURES

TABLE OF CONTENTS
(Continued)

LIST OF FIGURES

LIST OF SYMBOLS

Sections II A and II B:

C_i = $\dfrac{p_i - p_\infty}{1/2 \rho_\infty U_\infty^2}$ = pressure coefficient of i^{th} interface

j^2 = -1

k = $\dfrac{\omega b}{U}$ = reduced frequency

M = Mach number

$\bar{R}$ = defined by (11) [1]

$\bar{S}$ = defined by (11) [1]

U = free stream velocity

w = transverse displacement of panel

x, y, z = reference coordinate system

β = $(M^2 - 1)^{1/2}$

δ = boundary layer thickness

Γ = defined by (25) [1]

ρ = mass air density

Φ = chordwise deflection function

ω = frequency of vibration

$\bar{\omega}$ = $k \dfrac{M^2}{\beta^2}$

$( )^*$ = Laplace transform of ( )

Section II C:

x, y = cartesian coordinates

U_∞, M_∞ = velocity and Mach number of free stream

Section II C: (continued)

γ = ratio of specific heats

Φ = perturbation velocity potential divided by v_∞

φ = linearized potential due to Oswatitsch and Maeder

K = constant due to linearization of transonic flow equation

g = nonlinear correction term to φ

c* = location of sonic point on surface

c** = location of shock on surface

Y = discriminant of the root for g_x

α = $K/2\beta^2$

β^2 = $1 - M_\infty^2$

f_o = half amplitude to wave length ratio of sinusoidal wall

ω = angular frequency

N = $|\beta|/2f_o \cdot \varphi_x$

c_p = $-2\Phi_x$ = pressure coefficient

$$\bar{c}_p = -2\left[(\gamma+1)M_\infty^2\right]^{1/3} / (2f_o)^{2/3} \cdot \Phi_x$$

$$\xi_\infty = \left(M_\infty^2 - 1\right) / \left[(\gamma+1)M_\infty^2(2f_o)\right]^{2/3}$$

II. THEORETICAL CONSIDERATIONS

A. Panel Flutter of Low Aspect Ratio Panels

In [1], a new method has been developed for predicting the flutter boundaries for very low aspect ratio panels. The method is based on linearized, three dimensional potential flow theory and small deflection plate theory. In the analysis Laplace transform techniques are employed, which circumvent the need for introducing a large number of deformation functions such as in the Ritz-Galerbin method.

The solution of the panel flutter equations given in section IV of [1], however, requires the numerical evaluation of integrals of the form

$$\int_0^x e^{p_r(x-\xi)} e^{-j\bar{\omega}\xi} J_0(\Gamma\xi)\, d\xi$$

which, in practice, is expensive computational-wise for large values of x.

In this section, the situation is further explored and a more convenient way is given for solving the flutter equations.

The Laplace Transform of the panel flutter equations of motion, for a flat, rectangular panel with a pinned leading edge, is given by equation (74) of [1],

$$A\left\{\left[\left(p^2 - \frac{\pi^2}{4}\right)^2 - \bar{R}k^2 + \bar{S}\,\frac{(p+jk)^2}{\beta\left[(p+j\bar{\omega})^2 + T^2\right]^{1/2}}\right]\Phi^* - \left[p^2 - 2\left(\frac{\pi}{2}\right)^2\right]\Phi'(o) - \Phi'''(o)\right\}\cos\frac{\pi}{2}y = 0 \qquad (1)$$

Thus,

$$\varphi^* = \frac{A_1 \Phi'(o) + \Phi'''(o)}{A_2 + A_3 A_4^{-1}} \tag{2}$$

where

$$A_1(p) = p^2 - \frac{\pi^2}{2}$$

$$A_2(p) = \left(p^2 - \frac{\pi^2}{4}\right)^2 - \bar{R} k^2$$

$$A_3(p) = \frac{\bar{S}}{\beta} (p + jk)^2$$

$$A_4(p) = \left((p + j\bar{\omega})^2 + \Gamma^2\right)^{1/2}$$

To obtain the inverse Laplace transform of Φ^*, we write

$$\Phi^*(p) = \frac{\left\{B_1 + B_2 (A_4 - A_5)\right\} \Phi'(o) + \left\{B_3 + B_4 (A_4 - A_5)\right\} \Phi'''(o)}{C} \tag{3}$$

where

$$A_5(p) = p + j\bar{\omega}$$

$$B_1(p) = A_1 A_2 A_4 - A_1 A_3 A_5$$

$$B_2(p) = -A_1 A_3$$

$$B_3(p) = A_2 A_4^2 - A_3 A_5$$

$$B_4(p) = -A_3$$

and $$C(p) = A_2^{\,2} A_4^{\,2} - A_3^{\,2} \tag{4}$$

We assume that C (p) has ten distinct complex roots, $p_r (r = 1, 2, \cdots, 10)$.

Since $\left\{ \text{See [2], pp 237 (43)} \right\}$

$$L^{-1}\left\{A_4 - A_5\right\} = L^{-1}\left\{\left[(p + j\bar{\omega})^2 + \Gamma^2\right]^{1/2} - (p + j\bar{\omega})\right\}$$

$$= \frac{\Gamma\, e^{-j\bar{\omega}x}\, J_1(\Gamma x)}{x} \tag{5}$$

where J_1 is the Bessel Function of the first kind and first order, there follows

$$\Phi(x) = D_1(x)\ \Phi'(o) + D_2(x)\ \Phi'''(o) \tag{6}$$

where $$D_1(x) = L^{-1}\left\{\frac{B_1 + B_2 (A_4 - A_5)}{C}\right\}$$

$$= \sum_{r=1}^{10} \frac{B_1(p_r)}{C'(p_r)}\, e^{p_r x} + \sum_{r=1}^{10} \frac{B_2(p_r)}{C'(p_r)}\, I_r(x)$$

$$D_2(x) = \sum_{r=1}^{10} \frac{B_3(p_r)}{C'(p_r)}\, e^{p_r x} + \sum_{r=1}^{10} \frac{B_4(p_r)}{C'(p_r)}\, I_r(x)$$

and $$I_r(x) = \Gamma \int_o^x \frac{e^{p_r(x - \xi)}\, e^{-j\bar{\omega}\xi}\, J_1(\Gamma\xi)}{\xi} \tag{7}$$

It is useful for numerical evaluation to write $I_r(x)$ in another form.

Using the expression,

$$\frac{J_1(x)}{x} = \frac{2}{\pi} \int_0^1 (1 - t^2)^{1/2} \cos (x\, t)\, dt, \tag{8}$$

we can write

$$I_r(x) = \frac{2\,\Gamma^2}{\pi} \int_0^1 (1 - t^2)^{1/2} \left\{ \int_0^x e^{p_r(x - \xi)}\, e^{-j\bar{\omega}\xi} \cos\left\{\Gamma\, t\, \xi\right\} d\xi \right\} dt \tag{9}$$

where we have inverted the order of integration.

The inner integral can be computed and we find after a few manipulations,

$$\int_0^x e^{p_r(x - \xi)}\, e^{-j\bar{\omega}\xi} \cos\left\{\Gamma\, t\, \xi\right\} d\xi = (1/2) e^{p_r x} \left\{ (e_r + h_r) - j\,(g_r + h_r) \right\}$$

$$- 1/2\,(e_r - j\, g_r)\, e^{-j\,(\bar{\omega} - \Gamma\, t)\, x}$$

$$- 1/2\,(f_r - j\, h_r)\, e^{-j\,(\bar{\omega} + \Gamma\, t)\, x} \tag{10}$$

where

$$e_r(t) = \frac{a_r}{a_r^2 + (b_r + \bar{\omega} - \Gamma t)^2}$$

$$f_r(t) = \frac{a_r}{a_r^2 + (b_r + \bar{\omega} + \Gamma\, t)^2}$$

$$g_r(t) = \frac{b_r + \bar{\omega} - \Gamma\, t}{a_r^2 + (b_r + \bar{\omega} - \Gamma\, t)^2}$$

$$h_r(t) = \frac{b_r + \bar{\omega} + \Gamma t}{a_r^2 + (b_r + \bar{\omega} + \Gamma t)^2} \tag{11}$$

and

$$p_r = a_r + j b_r \tag{12}$$

Thus

$$I_r(x) = \frac{\pi^2}{\pi} \left[e^{p_r x} \int_0^1 \left\{ (e_r + f_r) - j (g_r + h_r) \right\} (1 - t^2)^{1/2} dt \right.$$

$$\left. - e^{-j \bar{\omega} x} \int_0^1 \left\{ (e_r - j g_r) e^{j \Gamma t x} + (f_r - j h_r) e^{-j \Gamma t x} \right\} (1 - t^2)^{1/2} dt \right] \tag{13}$$

To satisfy the boundary condition for a simply supported trailing edge, we will also need $\Phi''(x)$. This quantity is readily obtained by differentiating (6) twice with respect to x and we find,

$$\Phi''(x) = D_3(x)\ \Phi'(o) + D_4(x)\ \Phi'''(o) \tag{14}$$

where

$$D_3(x) = \sum_{r=1}^{10} \frac{B_1(p_r)}{C'(p_r)}\ p_r^2\ e^{p_r x} + \sum_{r=1}^{10} \frac{B_2(p_r)}{C'(p_r)}\ I_r''(x)$$

$$D_4(x) = \sum_{r=1}^{10} \frac{B_3(p_r)}{C'(p_r)}\ p_r^2\ e^{p_r x} + \sum_{r=1}^{10} \frac{B_4(p_r)}{C'(p_r)}\ I_r''(x) \tag{15}$$

and

$$I_r''(x) = \frac{\Gamma^2}{\pi} \left[p_r^2\ e^{p_r x} \int_0^1 \left\{ (e_r + f_r) - j (g_r + h_r) \right\} (1 - t^2)^{1/2} dt \right.$$

(See next page for continuation of formula.)

$$+ e^{-j\bar{\omega}x} \int_0^1 \left\{ (\bar{\omega} + \Gamma t)^2 (e_r - j g_r) e^{j\Gamma t x} \right.$$

$$\left. + (\bar{\omega} - \Gamma t)^2 (f_r - j h_r) e^{-j\Gamma t x} \right\} (1 - t^2)^{1/2} dt \Bigg] \tag{16}$$

The flutter condition is obtained in the usual way by satisfying boundary conditions at the trailing edge of the panel. For a simply supported trailing edge we must have

$$w = w'' = 0 \quad \text{at} \quad x = 2s \tag{17}$$

or

$$\Phi(2s) = \Phi''(2s) = 0 \tag{18}$$

The flutter condition becomes $\left\{ \text{see (6), (14) and (18)} \right\}$,

$$E = E_R + j E_I = D_1(2s) D_4(2s) - D_2(2s) D_3(2s) = 0 \tag{19}$$

The objective of this analysis is to obtain flutter boundaries for small aspect ratio panels ($s>>1$). The terms $e^{p_r x}$ in Equations (7), (13), (15) and (16), however, become very large when $Re(p_r)$ is positive and large, and $s>>1$, which could cause overflow in the computer. To circumvent this, we write

$$\Phi(x) = e^{\gamma x} \left[\bar{D}_1(x) \Phi'(o) + \bar{D}_2(x) \Phi'''(o) \right] \tag{20}$$

$$\Phi''(x) = e^{\gamma x} \left[\bar{D}_3(x) \Phi'(o) + D_4(x) \Phi'''(o) \right], \tag{21}$$

denote the root of $C(p)$ with the largest real part value by $p_s = a_s + j b_s$ and

let $\gamma = as$ (22)

The quantities $\bar{D}_1$, $\bar{D}_2$, $\bar{D}_3$ and $\bar{D}_4$ become

$$\bar{D}_1(x) = \sum_{r=1}^{10} \frac{B_1(p_r)}{C'(p_r)} e^{(p_r - \gamma)x} + \sum_{r=1}^{10} \frac{B_2(p_r)}{C'(p_r)} \bar{I}_r(x)$$

$$\bar{D}_2(x) = \sum_{r=1}^{10} \frac{B_3(p_r)}{C'(p_r)} e^{(p_r - \gamma)x} + \sum_{r=1}^{10} \frac{B_4(p_r)}{C'(p_r)} \bar{I}_r(x)$$

$$\bar{D}_3(x) = \sum_{r=1}^{10} \frac{B_1(p_r)}{C'(p_r)} p_r^2 e^{(p_r - \gamma)x} + \sum_{r=1}^{10} \frac{B_2(p_r)}{C'(p_r)} \bar{I}_r''(x)$$

$$\bar{D}_4(x) = \sum_{r=1}^{10} \frac{B_3(p_r)}{C'(p_r)} p_r^2 e^{(p_r - \gamma)x} + \sum_{r=1}^{10} \frac{B_4(p_r)}{C'(p_r)} \bar{I}_r''(x) \quad (23)$$

where

$$\bar{I}_r(x) = \frac{\Gamma^2}{\pi} \left[e^{(p_r - \gamma)x} \int_0^1 \left\{ (e_r + f_r) - j(g_r + h_r) \right\} (1 - t^2)^{1/2} dt \right.$$

$$\left. - e^{-(\gamma + j\bar{\omega})x} \int_0^1 \left\{ (e_r - j g_r) e^{j\Gamma t x} + (f_r - j h_r) e^{-j\Gamma t x} \right\} (1 - t^2)^{1/2} dt \right]$$

and

$$I_r''(x) = \frac{\Gamma^2}{\pi} \left[p_r^2 e^{(p_r - \gamma)x} \int_0^1 \left\{ (e_r + f_r) - j(g_r + h_r) \right\} (1 - t^2)^{1/2} dt - \right.$$

(See next page for continuation of formula.)

$$e^{-(\gamma + j\bar{\omega})x} \int_0^1 \left\{ (\bar{\omega} + \Gamma t)^2 (e_r - j g_r) e^{j\Gamma t x} + (\bar{\omega} - \Gamma t)^2 (f_r - j h_r) e^{-j\Gamma t x} \right\} (1 - t^2)^{1/2} dt \Bigg] \quad (24)$$

The flutter condition becomes

$$\bar{E} = \bar{E}_R + j \bar{E}_I = \bar{D}_1 (2s) \bar{D}_4 (2s) - \bar{D}_2 (2s) \bar{D}_3 (2s) \quad (25)$$

Once the flutter condition is satisfied, the flutter mode is given by

$$\Phi(x) = e^{\gamma x} \left[\bar{D}_1 (x) - \frac{\bar{D}_1 (2s)}{\bar{D}_2 (2s)} \bar{D}_2 (x) \right] ; \; 0 \leq x \leq 2s \quad (26)$$

The same procedure as given in [1] may be used to obtain flutter boundaries.

It is believed that the method outlined here will significantly reduce computation time for obtaining flutter boundaries.

It is remarked that the flutter analysis for low aspect ratio panels given in [1] and its solution given here are not restricted to the pinned edge case so that a treatment of the clamped edge case with in-plane loads is also possible.

B. Pressure Distribution on Wavy Walls with Turbulent Boundary Layer

Preliminary calculations have been made for the pressure distribution on stationary wavy walls with turbulent boundary layer using the methods given in [3] and [4]. Three experimental boundary layer velocity profiles of the 2 x 2 foot Ames tunnel were used in the analysis. The Mach number, M,

correlation number and boundary layer thickness, δ, of the profiles were

Profile No. 1: $M_\infty = 1.4$

Corr. No. 303-312

$\delta = .98$; $R_u = .98$

Profile No. 2: $M_\infty = 1.3$

Corr. No. 263

$\delta = 1.20$; $R_u = .98$

Profile No. 3: $M_\infty = 1.1$

Corr. No. 330

$\delta = 1.04$; $R_u = .98$

The boundary layer velocity profiles are given in Figure 1.

It was the purpose of the analysis to determine the perturbation pressure on a wavy wall surface of unit amplitude,

$$w_o = \sin \frac{2\pi x}{L}$$

The boundary layer was represented by ten sublayers of .2 inch thickness.

The perturbation pressures have been calculated in terms of the pressure coefficient for the i^{th} interface,

$$C_i = \frac{p_i - p_\infty}{(1/2)\rho_\infty U_\infty^2} = - A_i \sin\left(\frac{2\pi x}{L} - \varphi_i\right)$$

for wave lengths, L = 2, 6 and 10 inches. C_o is the pressure coefficient for the surface of the wavy wall.

The pressure amplitude, A_o, and phase angle φ_o, has been plotted

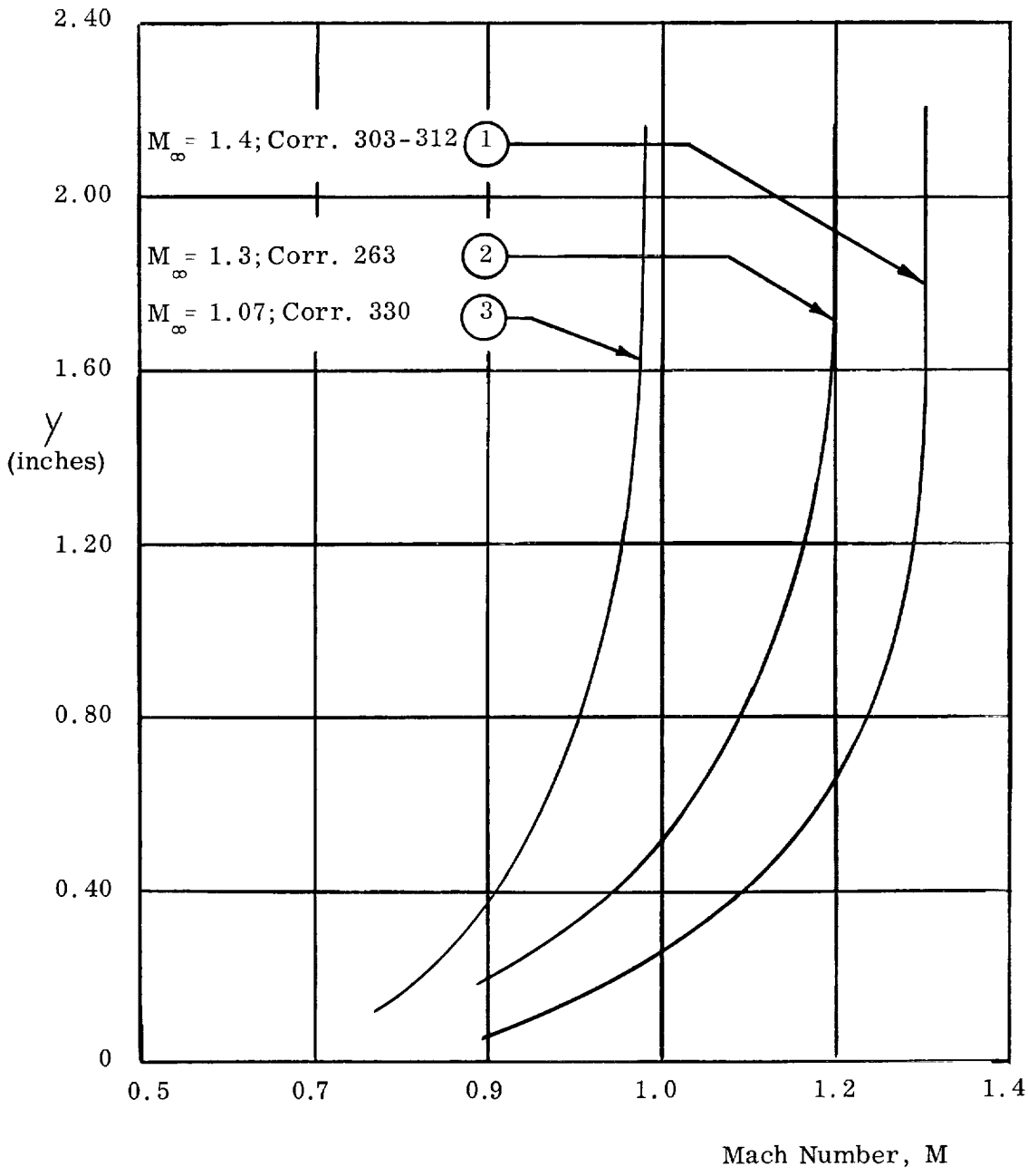

Figure 1. NASA Ames Boundary Layer Velocity Profiles.

versus wave length L for the three profiles in Figure 2. The zero boundary layer thickness case is also shown in the graph.

It is interesting to observe that with respect to the zero boundary layer thickness case, the $M_\infty = 1.40$ profile results in an amplification of pressure amplitude while the $M_\infty = 1.07$ profile gives an attenuation. In all cases, the boundary layer causes a forward phase shift which becomes progressively larger with decreasing wave length. This is to be expected, since the ratio of boundary layer thickness and wave length increases.

The pressure variation through the boundary layer is given in Figures 3, 4, 5, for Profile No. 1, $M_\infty = 1.4$, and L = 2, 6 and 10 respectively. A typical line of constant pressure is also shown in the graphs.

C. Inviscid Transonic Small Disturbance Theory

A new method for treatment of the nonlinear problem of transonic flow past an infinite sinusoidal wall has been given by Hosokawa [6]. Inasmuch as the present problem of low supersonic boundary layer flow on wavy walls contains to a limited extent transonic perturbations, it is felt that examination of Hosokawa's results for the stationary wavy wall may at least serve to point out the limitations and short-comings of a linearized theory representation of the boundary layer flow and hopefully initiate a study of a method for correcting the linear theory.

Hosokawa treats the two-dimensional, inviscid, transonic flow past stationary sinusoidal walls continuously through the transonic range. The basic transonic equation is given as:

$$(1 - M_\infty^2)\,\Phi_{xx} + \Phi_{yy} = (\gamma + 1) M_\infty^2\,\Phi_x \Phi_{xx} \tag{27}$$

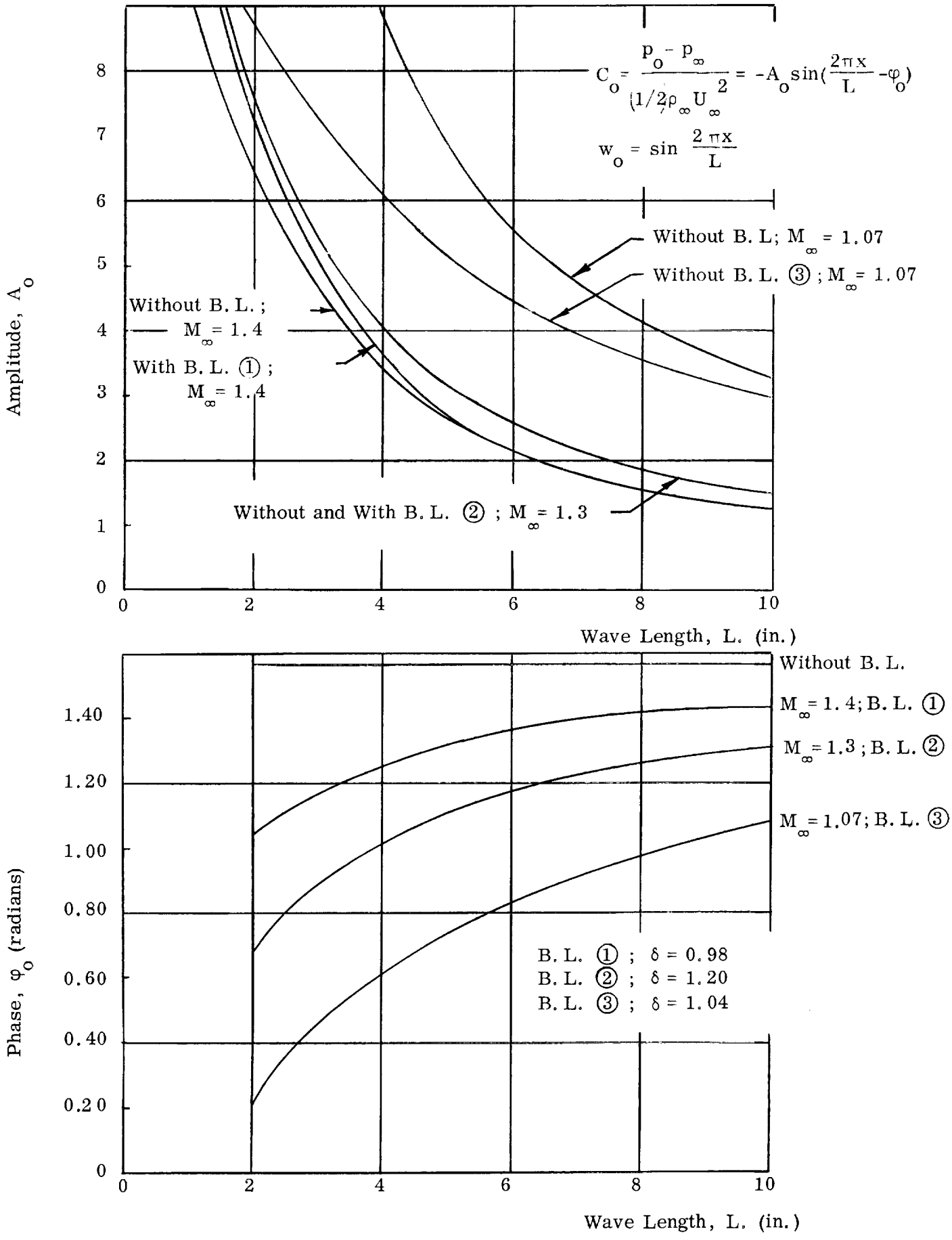

Figure 2. Pressure coefficient Versus Wave Length.

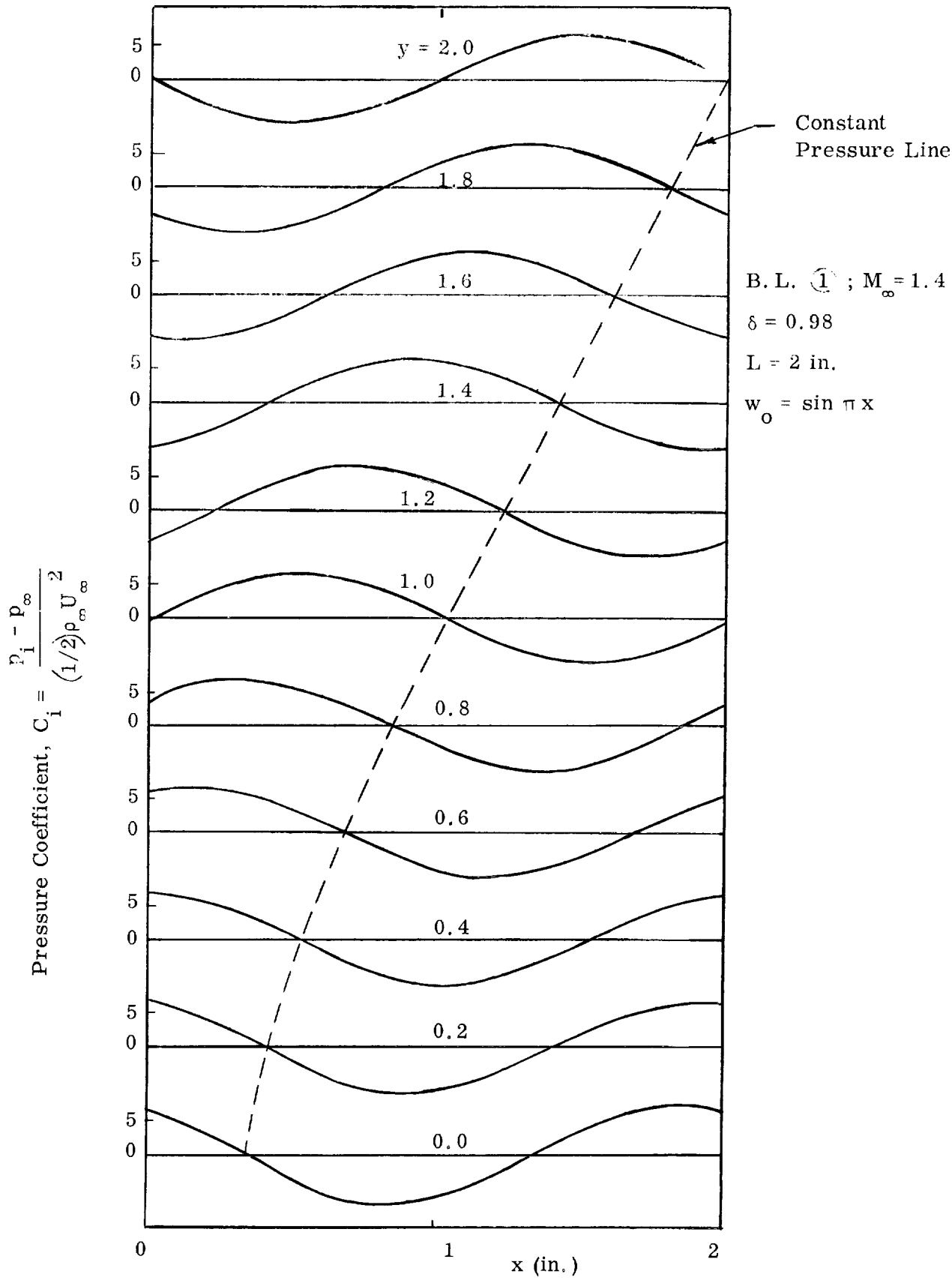

Figure 3. Pressure Variation Through Boundary Layer, L = 2".

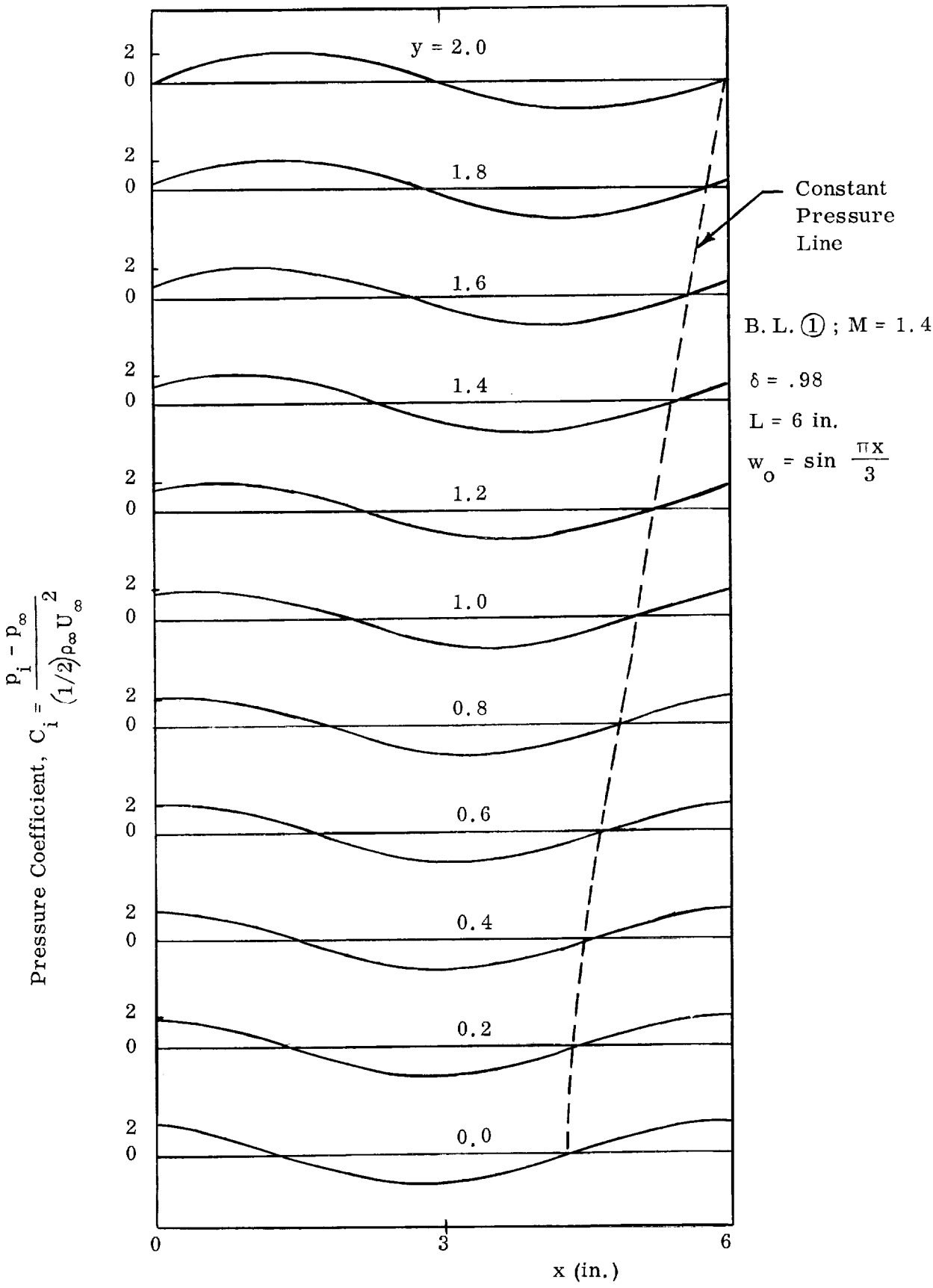

Figure 4. Pressure Variation Through Boundary Layer, L = 6"

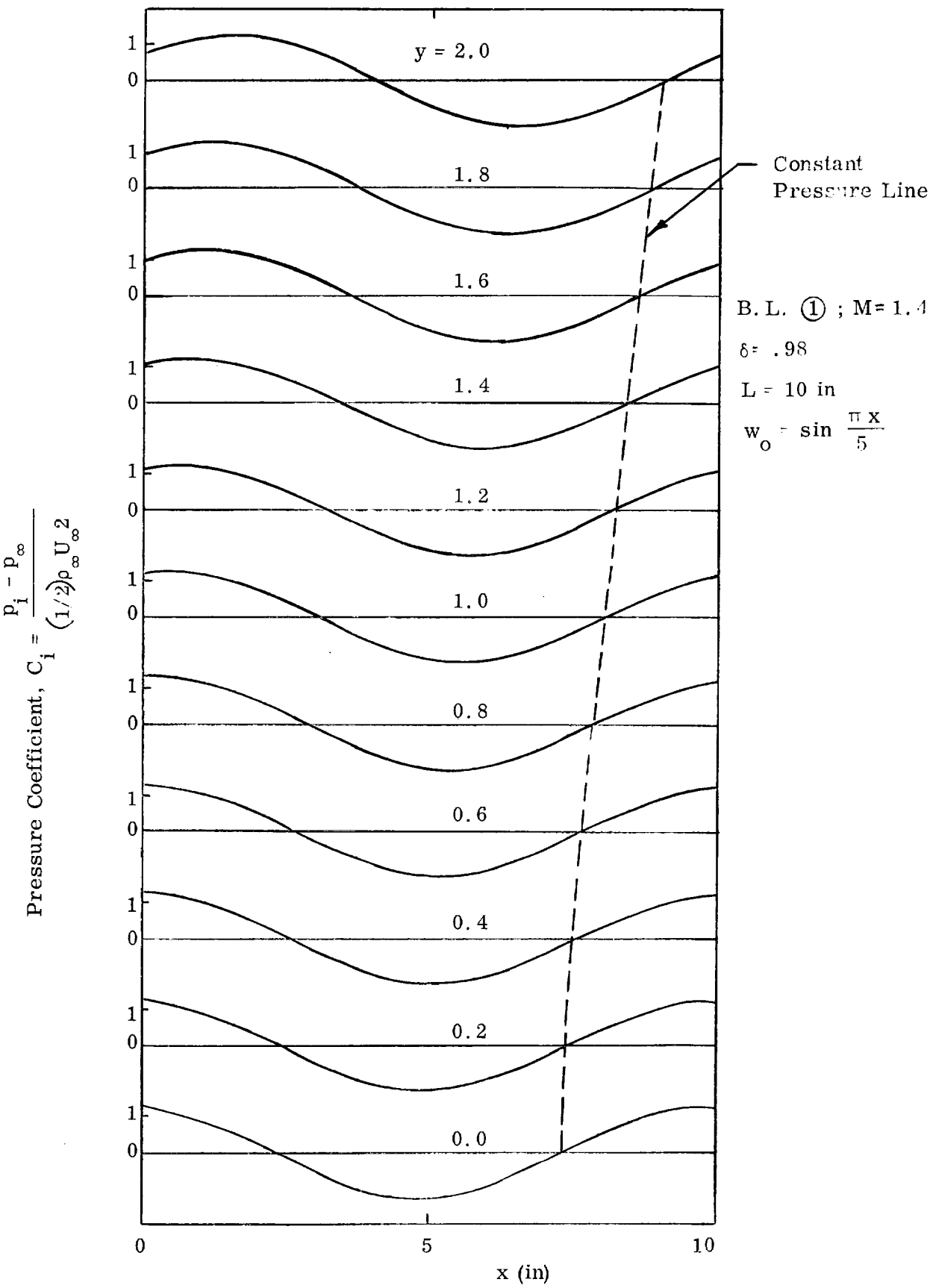

Figure 5. Pressure Variation Through Boundary Layer, L = 10"

where $U_\infty \Phi$ is the perturbation velocity potential. By defining

$$\Phi = \varphi + g \tag{28}$$

the approximate potential φ satisfies the linearized equation

$$(1 - M_\infty^2)\, \varphi_{xx} + \varphi_{yy} = K \varphi_x \tag{29}$$

which together with the boundary conditions

$$\left.\begin{aligned} \varphi_y &= i\omega f_o\, e^{i\omega x} \quad \text{at } y = 0 \\ \text{grad } \varphi &\to 0 \quad \text{as } y \to \infty \end{aligned}\right\} \tag{30}$$

for a wavy wall

$$f(x) = f_o e^{i\omega x} \tag{31}$$

yields the solution

$$\varphi = - \frac{i\omega f_o}{\mu} \exp(-\mu y + \omega x) \tag{32}$$

with

$$\mu = (\beta^4 \omega^4 + K^2 \omega^2)^{1/4} \exp(i/2 \tan^{-1} K/\beta^2 \omega) \tag{33}$$

$$\beta^2 = 1 - M_\infty^2 \tag{34}$$

and K an appropriately chosen constant.

The equation governing the nonlinear correction term g is established from equations (27)- (29) and satisfied approximately in the neighborhood of the wall by neglect of a small order term g_{yy}. The result at the wall (y = 0) is:

$$g_x = -\varphi_x + \frac{(1 - M_\infty^2)}{(\gamma + 1)M_\infty^2} \pm \sqrt{Y(x)} \tag{35}$$

where

$$Y(x) = \left\{\varphi_x - \frac{1 - M_\infty^2}{(\gamma + 1)M_\infty^2}\right\}^2 - 2\int_{c^*}^{x} \left\{\varphi_{xx} - \frac{K}{(\gamma + 1)M_\infty^2}\right\}\varphi_x dx \tag{36}$$

with the double sign corresponding to

$$\varphi_x \gtrless \frac{(1 - M_\infty^2)}{(\gamma + 1)M_\infty^2} \tag{37}$$

The location of the sonic point c^* and the value of K are determined uniquely as:

$$\varphi_x(x = c^*,\ y = 0) = \frac{(1 - M_\infty^2)}{(\gamma + 1)M^2} \tag{38}$$

$$\varphi_{xx}(x = c^*,\ y = 0) = \frac{K}{(\gamma + 1)M_\infty^2} \tag{39}$$

Equations (38) and (39) constitute the simultaneous equations for c^* and K for transonic flows; whereas for purely subsonic or supersonic flows the value of c^* is fixed at its lower or upper critical values respectively and K is determined by equation (39).

If the expression for the linearized flow velocity is written as

$$\varphi_x = \frac{2f_o}{|\beta|} N(x;\ \xi_\infty) \tag{40}$$

with ξ_∞ the reduced free stream Mach number

$$\xi_\infty = \frac{M_\infty^2 - 1}{\left[(\gamma + 1) M_\infty^2 (2f_o)\right]^{2/3}} \tag{41}$$

and the approximate relation

$$c_p = -2\Phi_x \tag{42}$$

is rewritten in reduced form as

$$c_p = \frac{\left[(\gamma + 1) M_\infty^2\right]^{1/3}}{(2f_o)^{2/3}} \, \bar{c}_p \tag{43}$$

then the following expression for $\bar{c}_p$ is obtained with the aid of equations (28), (33), (35), and (40):

$$c_p = -2 \left\{ (\pm)_1 |\xi_\infty| \pm \sqrt{2} \left[|\xi_\infty|^2 (\pm)_1 |\xi_\infty|^{1/2} N(x) + 2 |\alpha| \, |\xi_\infty|^{1/2} \int_{c^*}^{x} N(x) \, dx \right]^{1/2} \right\} \tag{44}$$

with

$$\alpha = \pm \pi \sqrt{\frac{\pi^{4/3}}{\xi_\infty^2}} - 1 \tag{45}$$

for $|\xi_\infty| \leq \pi^{2/3}$ where the double signs with and without the parenthesis $(\,)_1$ correspond respectively to $M_\infty \lessgtr 1$ and $N(x) \, (\pm)_1 |\xi_\infty|^{3/2} \gtrless 0$.

For $|\xi_\infty| \geq \pi^{2/3}$ equation (44) simplifies to

$$\bar{c}_p = -2\left\{(\pm)_1 |\xi_\infty| \pm \left[|\xi_\infty|^2 + N(c^*)^2 |\xi_\infty|^{-1} \right.\right.$$

$$\left.\left. (\bar{+})_1 2 |\xi_\infty|^{1/2} N(x)\right]^{1/2}\right\} \tag{46}$$

Corresponding to $|\xi_\infty| \leq \pi^{2/3}$ the flow is transonic (i.e., mixed) and half of the pressure jump at the shock is found from (44) to be

$$\frac{\Delta \bar{c}_p}{2} = 2\sqrt{2}\left[|\xi_\infty|^2 (\bar{+})_1 |\xi_\infty|^{1/2} N(c^{**}) + 2|\alpha| |\xi_\infty|^{1/2} \int_{c^*}^{c^{**}} N(x)\,dx\right]^{1/2} \tag{47}$$

The shock position c** and the sonic point c* are determined as the roots of equations (38) and (39) and are given by

$$\cos\left[4\pi c^*\right] = -\frac{\xi_\infty}{\pi^{2/3}} \tag{48}$$

and

$$\cos\left[2\pi c^{**} - 1/2 \tan^{-1}\left(\pm\sqrt{\frac{\pi^{4/3}}{\xi_\infty^2} - 1}\right)\right] = -\frac{\xi_\infty}{\pi^{2/3}} \tag{49}$$

Hosokawa's method has been programmed and computation carried out on the Georgia Tech Burroughs B-5500 digital computer for the three wall amplitude to wave length ratios $\epsilon/L = 0.005, 0.010, 0.015$. Each wall pressure distribution is considered for Mach numbers $M_\infty = 0.8, 0.9, 0.95, 1.05, 1.1, 1.2$, and 1.3.

As a matter of interest preliminary calculations have been made for the reduced free stream Mach number vs. free stream Mach number for the three wall amplitudes of interest (Figure 6), wall amplitude to wave length ratio vs. free stream Mach number for the critical conditions $\xi_\infty = \pm \pi^{2/3}$ (Figure 7.), and the sonic point, shock location, and shock strength vs. reduced free stream Mach number (Figure 8). In both Figures 6 and 7 the range of transonic or mixed flow is clearly shown as it depends on Mach number, M_∞ or ξ_∞, and wall amplitude ϵ/L. In Figure 8 the regions of subsonic and supersonic flow on the wall are shown together with the shock strength and position.

The pressure distributions for the various Mach numbers chosen are shown in Figures 9, 10, and 11 for the wall amplitude to wave length ratios of 0.005, 0.010, and 0.015 respectively. For comparison the analogous peak pressures predicted by linearized subsonic and supersonic theory are also shown. Whereas the magnitudes of the linearized theory predictions are reasonable for free stream Mach numbers sufficiently far removed from $M = 1$, the phase or location of the peak pressures and the consequent shape of the pressure distributions are in obvious disagreement with the transonic theory.

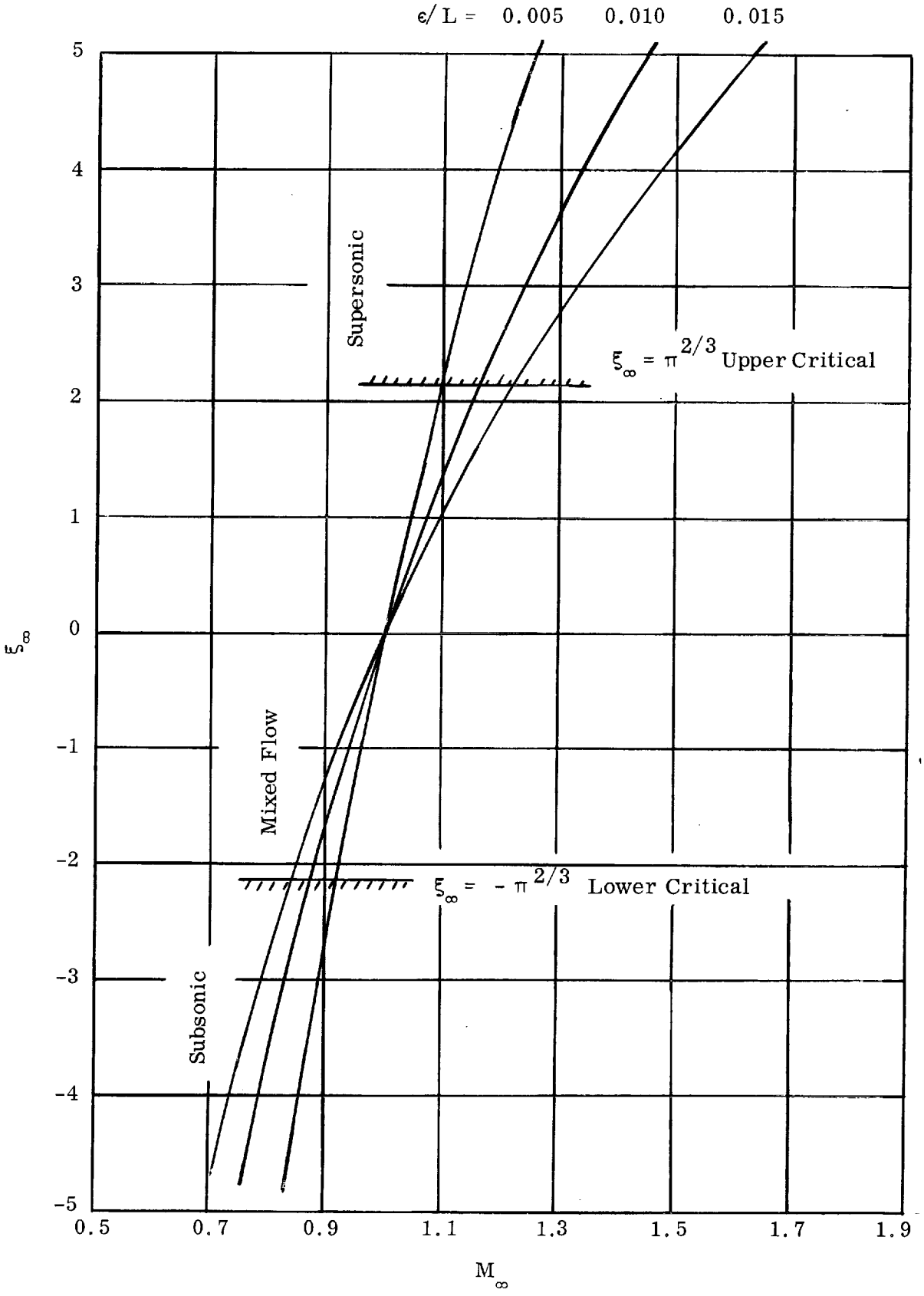

Figure 6. Reduced Mach No. ξ_∞ vs. Mach Number M_∞.

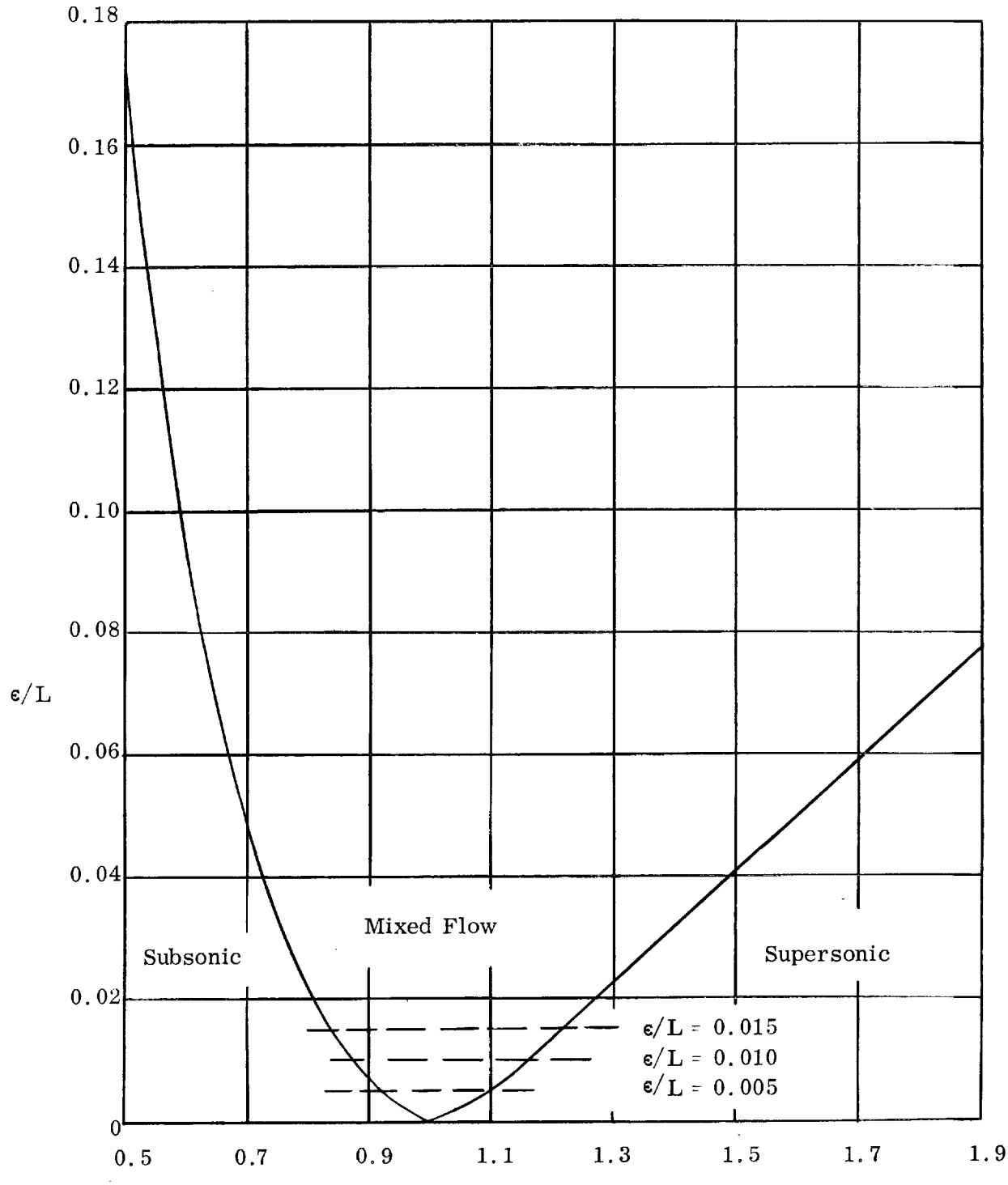

Figure 7. Critical Mach No. $M_{\infty\,crit}$ vs. Wall Amplitude Ratio ϵ/L.

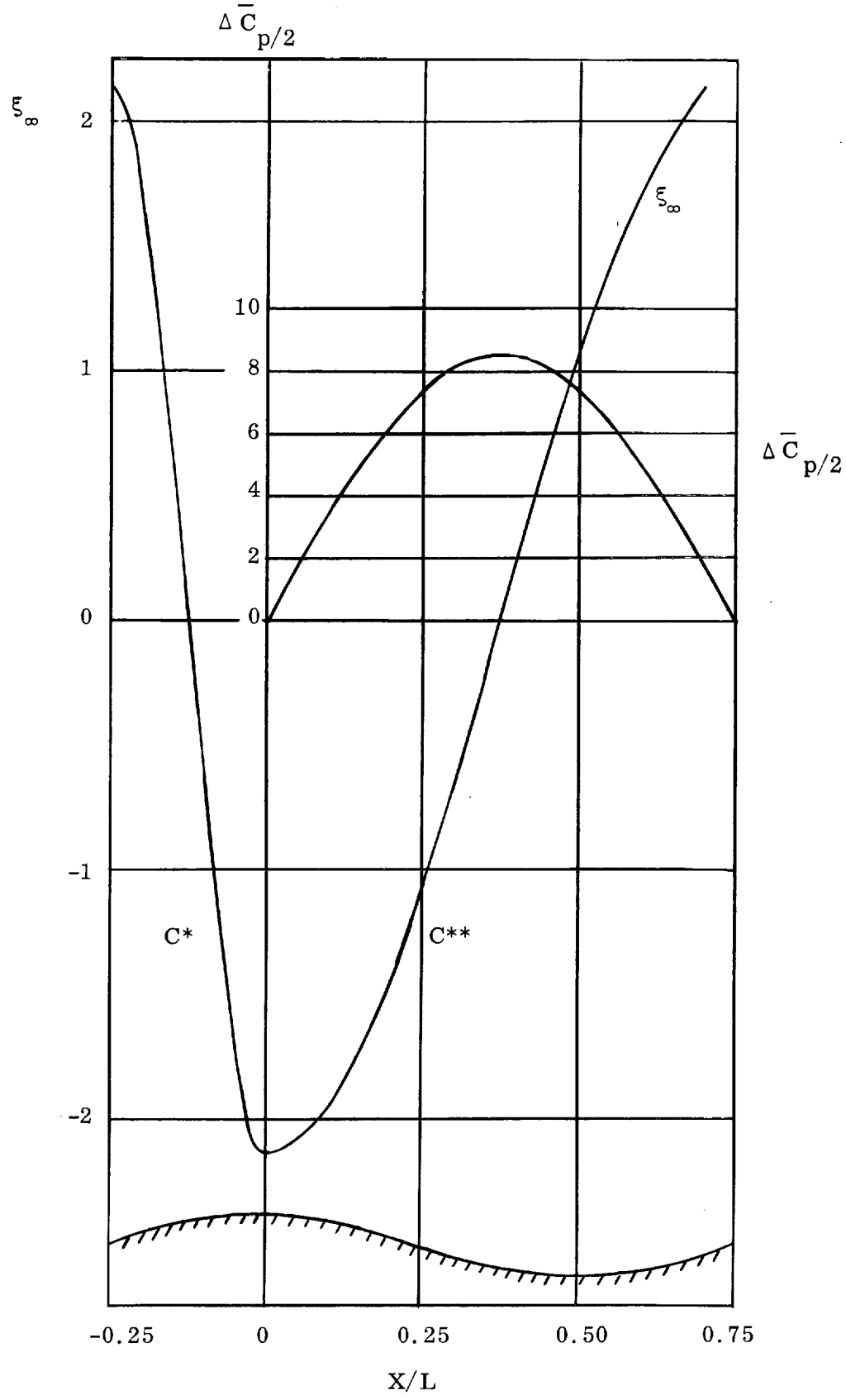

Figure 8. Sonic Point, Shock Point, and Shock Strength vs. Reduced Mach Number.

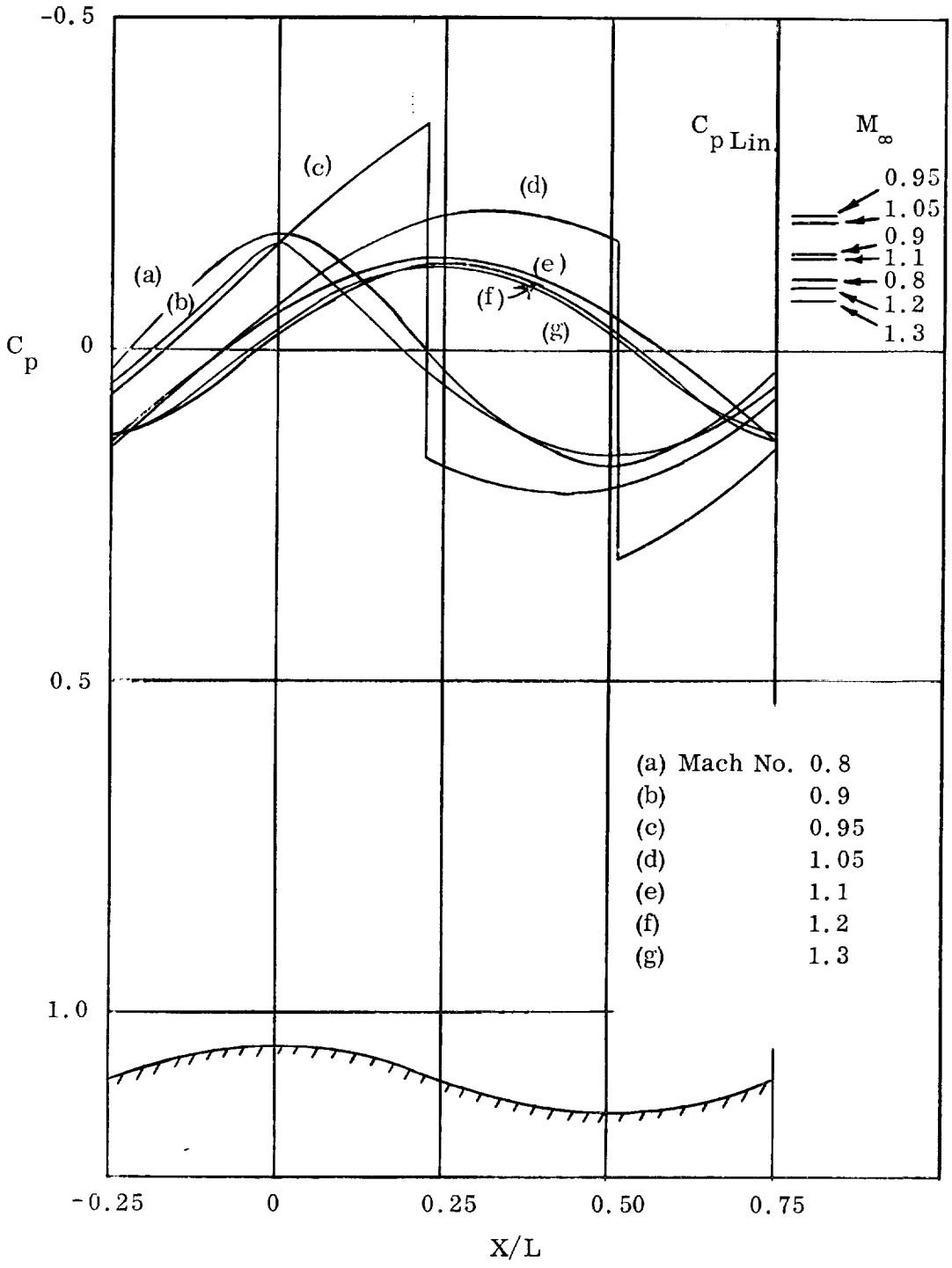

Figure 9. Pressure Distribution $\epsilon/L = 0.005$.

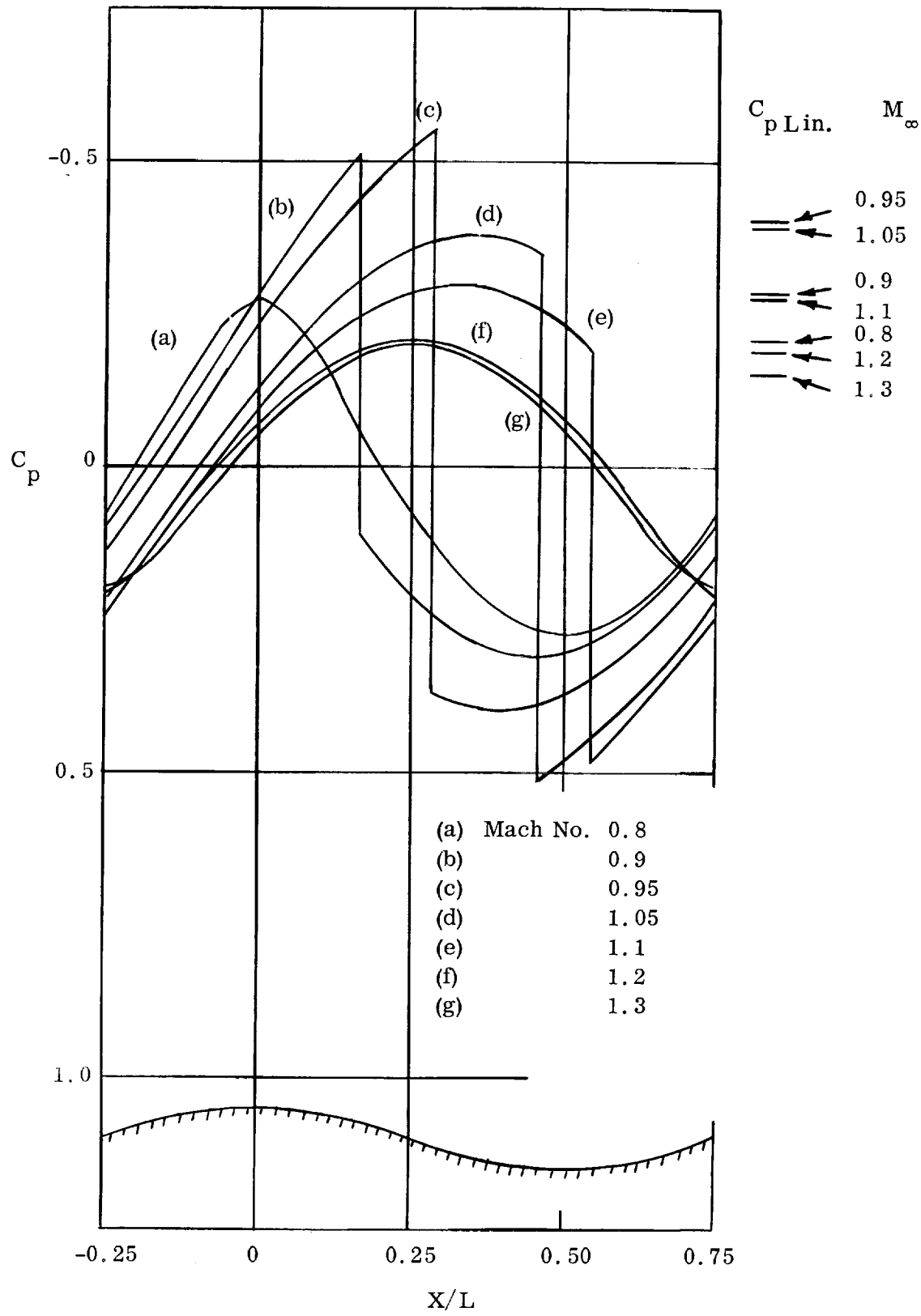

Figure 10. Pressure Distribution $\epsilon/L = 0.010$.

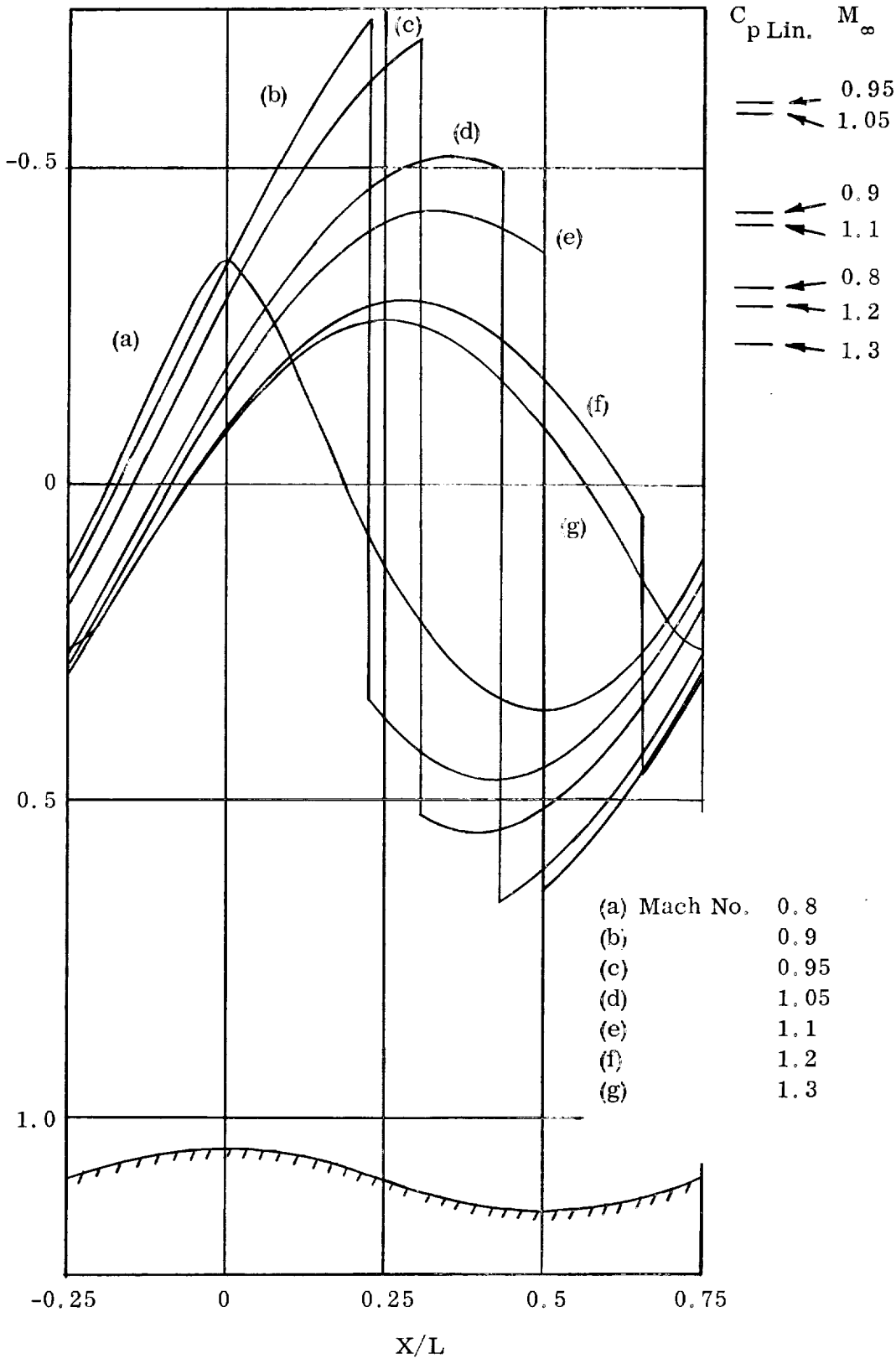

Figure 11. Pressure Distribution $\epsilon/L = 0.015$.

III. EXPERIMENTAL INVESTIGATION

The prime objective of the experimental investigation is to gather information on the pressure distribution of two dimensional sinusoidal wavy walls in low supersonic flow with turbulent boundary layer. To enhance comparison with theoretical analysis, it is desired to measure the perturbation pressures on the surface and within the turbulent boundary layer of variable thickness.

Much of the work concerning the selection of suitable model parameters and the design of the boundary layer probe has been accomplished under a preceeding contract [1]. The main efforts during the course of this program were directed towards the final selection and fabrication of the models, the fabrication of the boundary layer probe and the gathering of experimental data.

A. Wind Tunnel Models

The wind tunnel models consisted of five two-dimensional wavy wall models with 2 ft. span manufactured by the NASA, Marshall Space Flight Center. The configurations of the models are given in the following table.

Model Number	Wave Length (Inches)	Half Amplitude (Inches)	Fineness Ratio	Total Number of Waves
A	6	0.090	0.015	5
B	6	0.060	0.010	5
C	6	0.030	0.005	5
D	2	0.010	0.005	16
E	10	0.050	0.005	3

It was the intension to study fineness ratio effects with model A, B and C and wave length effects with model C, D and E.

The models were constructed from 1" aluminum blocks and were made to fit the splitter plate configuration of the 2 x 2 foot Ames tunnel.

The machined surface of the models was hand polished to a smooth wavy surface and the tolerance of the finished product was held to within ± .001 inches over the entire surface.

All models were instrumented with three rows of static pressure orifices; one along the center line of the model and one on either side six inches away from the center line row. All orifices were drilled perpendicular to the wavy wall surface and had a diameter of .032 inches. The number and location of the orifice was the same for each row. There were either seventeen or five equally spaced orifices along a wave. The waves with seventeen orifices were; for models A, B and C, the first, third and fifth; for model D, the first, fifth, eleventh and fifteenth and for model E, the first, second and third. In addition, six orifices were placed along the leading edge of each row.

B. Boundary Layer Probe

A general description of the boundary layer probe is given in [1]. The probe was sting supported and designed to move in three mutually perpendicular directions for survey measurements of the boundary layer pressure and velocity distributions. In order to minimize tunnel blockage, the maximum cross sectional area of the probe mechanism was kept at 1.5 per cent of the cross-sectional area of the test section. To prevent flow disturbance, all tubular sections were terminated in cones and all other sections in wedges with maximum included angle of 16 degrees. Photographs of the boundary layer probe installed in the 2 x 2 ft. transonic wind tunnel at Ames are given in Figures 13, 14 and 15.

During the course of the program extreme difficulties were experienced with the fabrication of the inboard wing structure. The sliding keys introduced

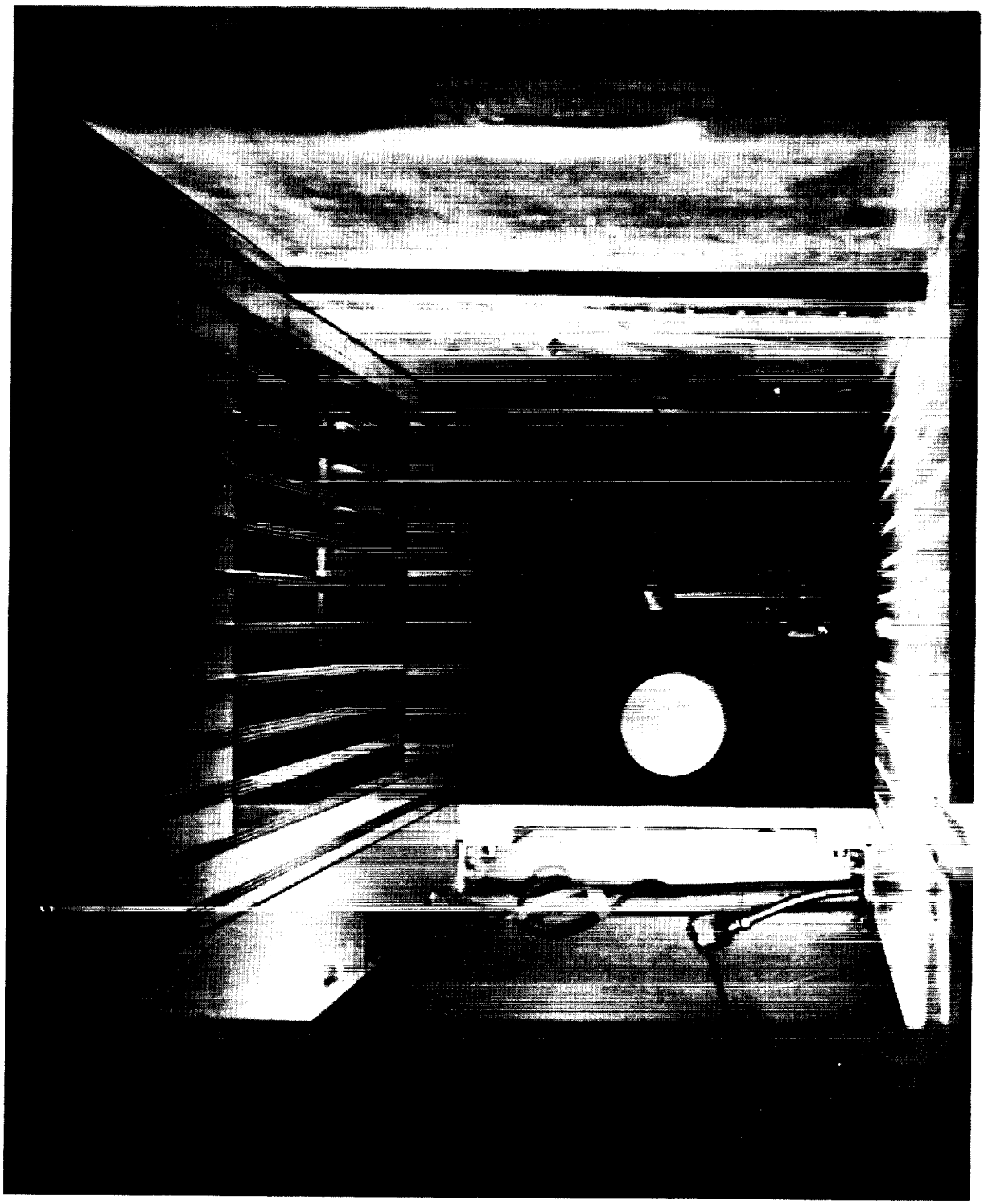

Figure 12. Front View of Boundary Layer Probe Installed in the 2 by 2 foot Transonic Wind Tunnel at Ames.

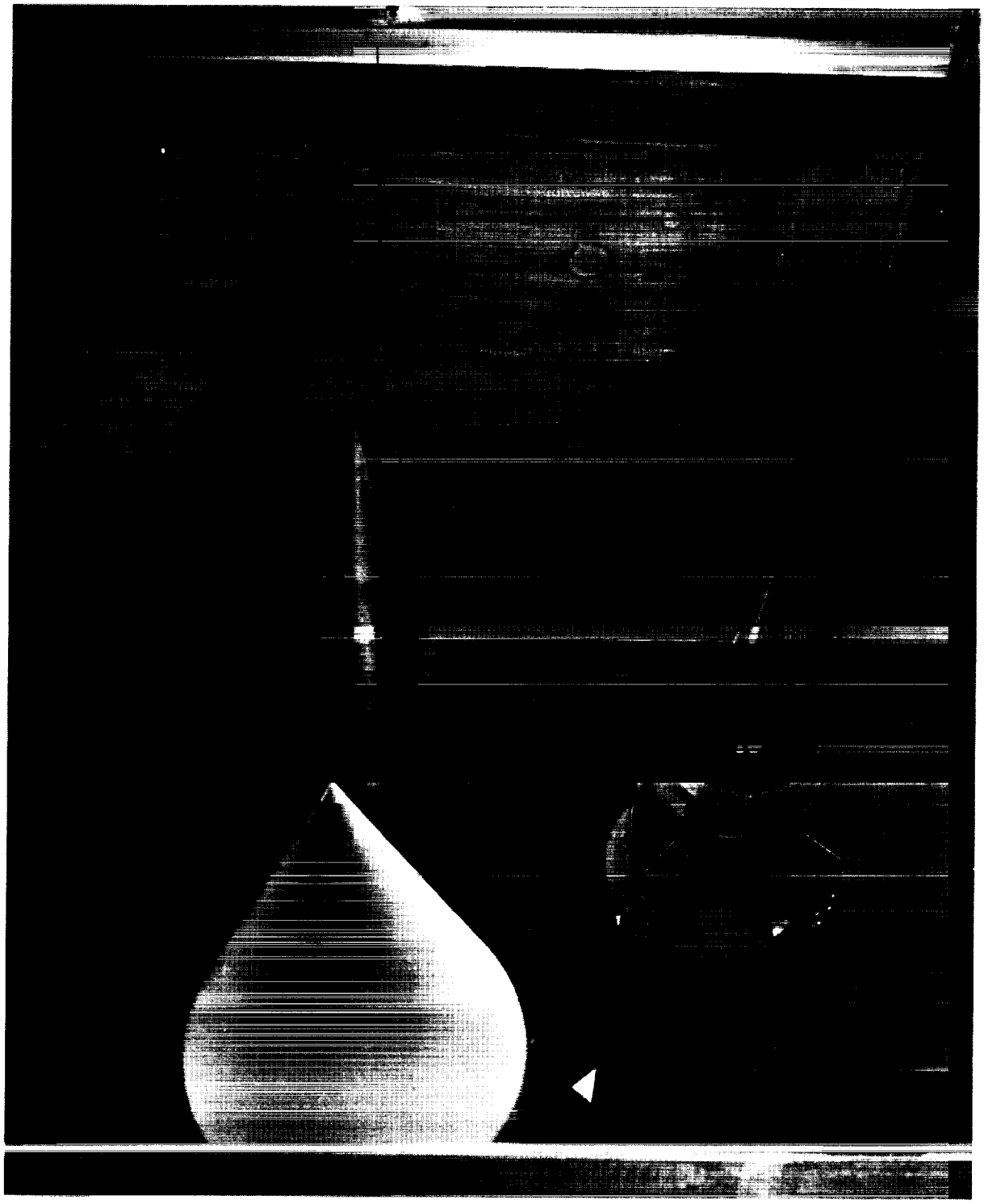

Figure 13. Three Quarter Front View of Boundary Layer Probe in Fully Retracted Position Installed in the 2 by 2 foot Transonic Wind Tunnel at Ames.

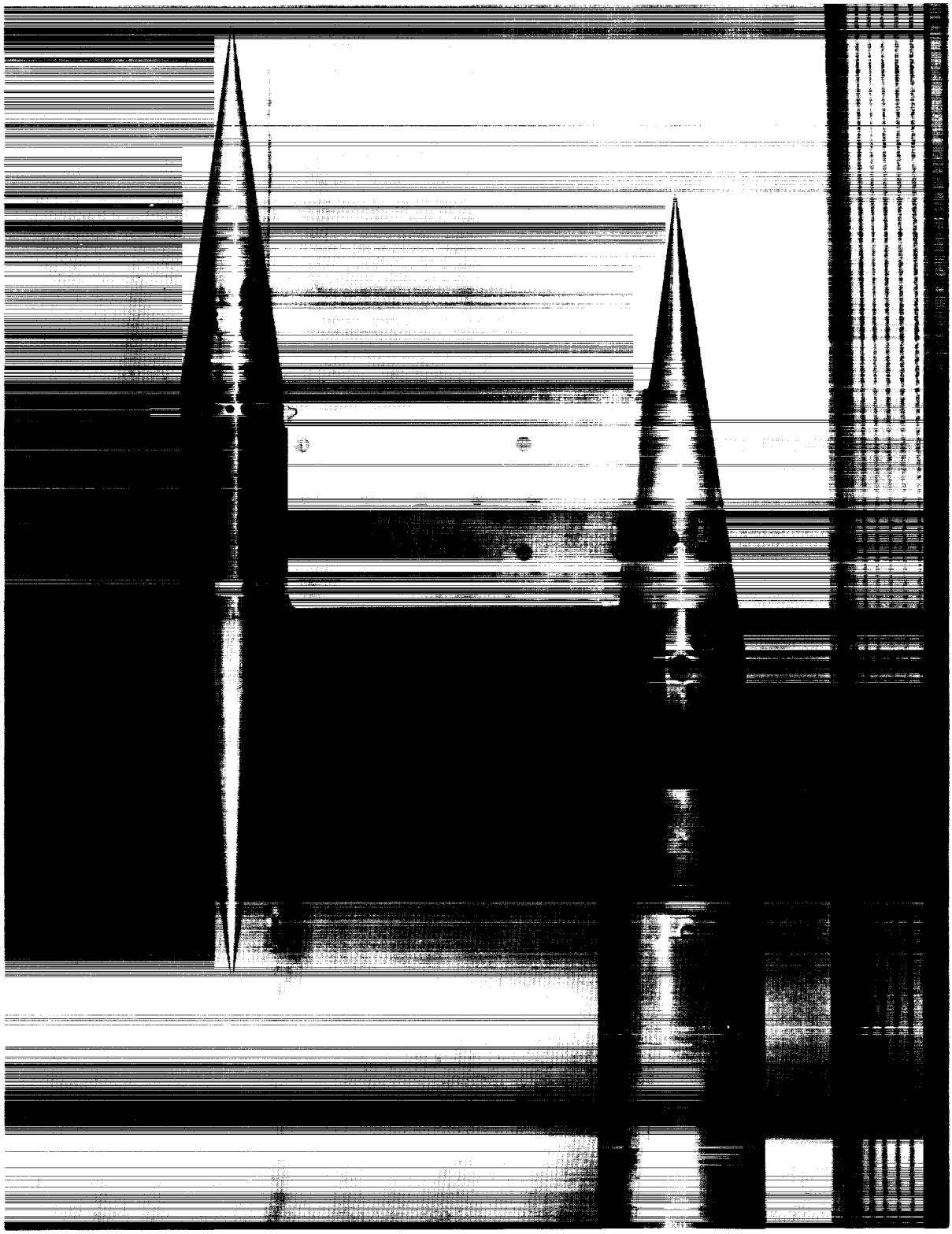

Figure 14. Side View of Boundary Layer Probe in Partially Extended Position Installed in the 2 by 2 foot Transonic Wind Tunnel at Ames.

caused considerable binding when load was applied. Various improvements of the keys were tried but without success. It became apparent that a redesign of the inboard wing section was necessary. In order to simplify matters it was proposed to relax the requirement on cross-sectional area and to increase the inboard wing thickness. Adequate information on the effects of model cross-sectional area on the flow conditions of the 2 x 2 ft. tunnel, however, was not available, and it was decided to conduct the two dimensional wavy wall tests with the inboard wing section fixed in mid-position. The possibility of increasing cross-sectional area could then be investigated during the tests.

During the fabrication phase of the probe a large number of minor modifications have been made to enhance the overall performance of this instrument. These modifications are not reported here but have been incorporated in the final set of working drawings which are submitted together with this report.

A structural integrity analysis of the boundary layer probe is also given in [1]. A few minor changes to that analysis had to be made, however, for the fixed inboard strut case. The final stress analysis for the probe with retracted inboard strut have been submitted to the Marshall Space Flight Center and the Ames Research Center on March 28, 1966.

In addition to these analysis a flutter analysis for the wing sections of the probe has been conducted. These analysis were based on the simplified two dimensional parametric studies of Garrick and Rubinow [5]. The results of these calculations are given in Figure 12 which illustrates the non-dimensional flutter speed $U_F/b\omega_\alpha$ versus Mach number, M , for the inboard and outboard

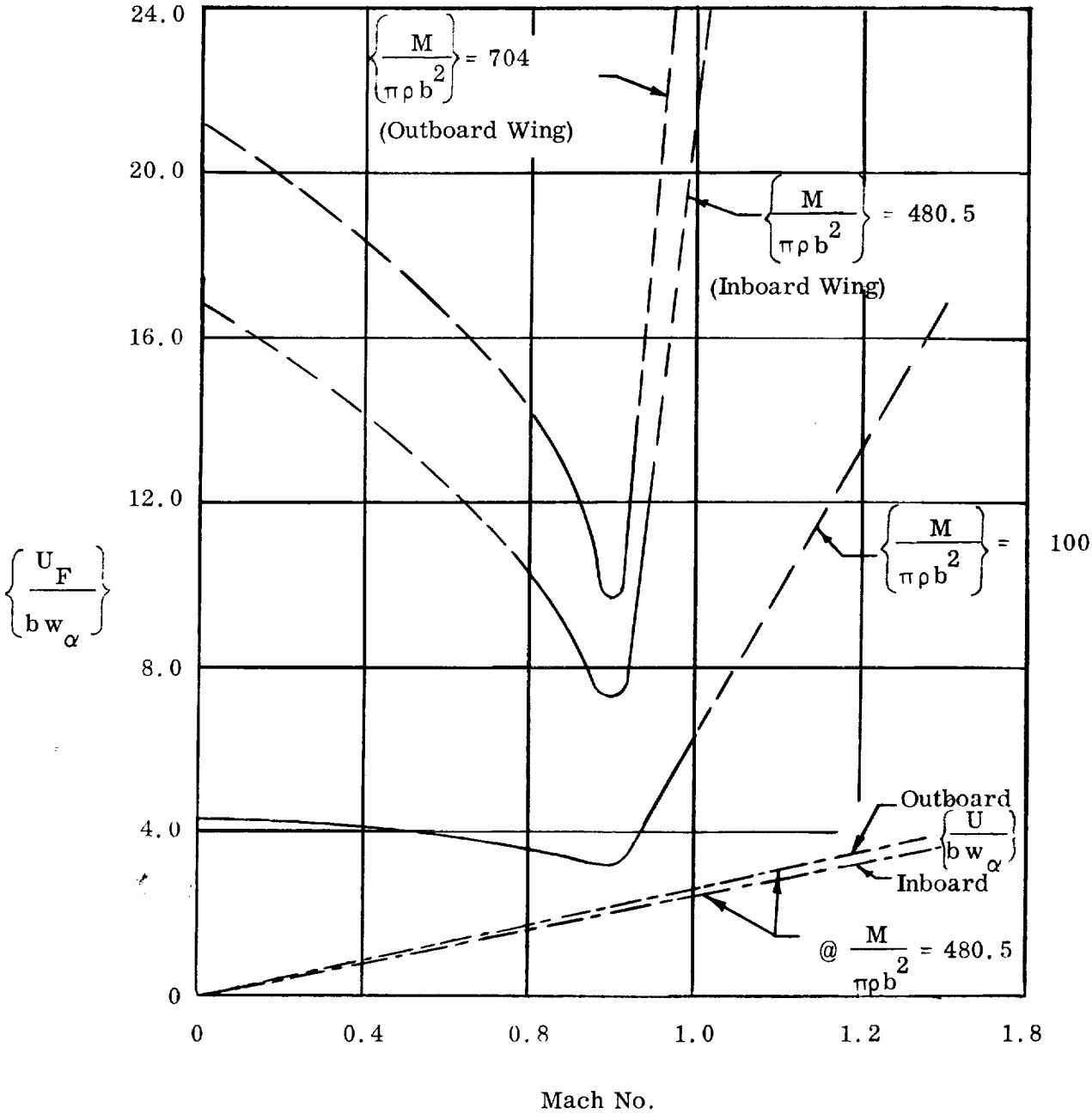

Figure 15. Dimensionless Bending-Torsion Flutter Speed Versus Mach Number. Inboard and Outboard Wing Section.

wing sections. The straight lines through the origin,

$$\frac{U}{b\omega_\alpha} = \frac{a_\infty}{b\omega_\alpha} M$$

which characterize the flight conditions for the sections at sea level are also shown in the graph. It is seen that there is a considerable margin of safety with respect to flutter. This is to be expected since the probe was designed for small deflection under load.

Preliminary tests have been conducted at Georgia Tech to evaluate the overall performance of the probe at various stages of design. During these tests aerodynamic loads, particularly the drag loads, were simulated.

The boundary layer probe with the inboard wing strut in locked retracted position was delivered to the Ames Research Center on March 8, 1966.

C. Wind Tunnel Investigation

The two dimensional wavy wall tests were conducted in the 2 x 2 ft. transonic research tunnel of the NASA Ames Research Center. The collection of experimental information was directed by Ames personnel.

The tests have been run during the period of June 1966 through September 1966. At present, the data collected is being prepared for further investigation. Since it has been decided to conduct the data analysis under a future contract, only a brief summary of the wind tunnel experiments will be given here.

The models were bolted to the splitter plate which was mounted on one of the side walls of the tunnel. The splitter plate is designed to vary the turbulent boundary layer thickness over the surface of the model. The maximum and minimum boundary layer thicknesses which can be obtained are approximately 2 and .4 inches.

The probe was attached to the sting and a rear mount in the diffusor section of the tunnel. The probe alignment in the tunnel was checked with respect to the tunnel axis and the splitter plate plane.

The static pressures on the surface of the models were measured automatically by means of a scani-valve arrangement and a Beckman computer. Further reduction of the data was done on a IBM 7094 computer.

A total and static pressure probe was used to measure boundary layer velocity profiles. The probe could be traversed through a distance of 3 inches normal to the model surface and through a distance of 60 inches in the axial direction. The boundary layer was automatically traversed while taking pressure readings at 25 positions. The axial position was controlled manually.

Prior to the wavy wall tests a flutter test was conducted for the boundary layer probe. The probe was placed at approximately mid position of the tunnel test section and a calibration plate was installed on the splitter plate. The overall vibration levels were measured by means of an accelerometer which was located in the motor pod. The wing motions were observed through the tunnel window. The general testing procedure was to first sweep through the tunnel Mach number range $.6 \leq M \leq 1.4$ at low dynamic pressure, q, and then to increase q.

It was found that the probe was flutter free within the region of tunnel capability. In the transonic region, however, particularly near $M = .85$, excessive vibration of the probe tip occurred due to tunnel turbulence. These vibrations, which were predominantly in a plane parallel to the splitter plate plane, were reduced to an acceptable level (approximately 1/32 of an inch) by stiffening the probe tips of both the static and total pressure probes.

values of Mach number, Reynolds number and splitter plate position, all

The following data was collected during the tests.

For the models A-C, the static pressures on the model surface was measured at M = 0.8, 0.9, 0.95, 1.1, 1.2, 1.3 and 1.35 with q ~600 p.s.f. and a splitter plate position of 0.0, 0.2, 0.5 and 1.0 inch away from the tunnel wall.

The models C, D and E were used for a Reynolds number check. Surface pressures were measured at M = 0.8, 0.95 and 1.2 with the same splitter plate positions and two values of dynamic pressure higher than q = 600 p.s.f.

Data on boundary layer velocity profile and boundary layer thickness was obtained with the probe at M = 1.2, 1.3 and 1.35 and q ~600 p.s.f. For the flat calibration plate, this information was collected at various distances from the leading edge of the splitter plate with a total pressure probe. Boundary layer profiles for the models C and D were obtained at the leading and trailing edge of the model and along a fully instrumented wave in the vicinity of the middle of the model. In the latter case, total and static pressures were measured at the same location through the boundary layer.

It is intended to use four surface mounted total pressure probes of the Ames Research Center to obtain boundary layer information at M < 1.2. This data will be obtained during a future test for the calibration plate only.

During the tests a cursory evaluation of the experimental data was performed. The data shows no signs of separation or the presence of strong shocks. This was true even for model A which had the largest amplitude to wave length ratio. The effects of non linearity in the pressure distribution were in general small. A pronounced non linear pressure distribution was

only observed close to M = 1 and at the larger amplitude to wave length ratios. In all cases examined, the boundary layer introduced an attenuation in pressure amplitude and an upstream phase shift. This is in agreement with theoretical predictions. The data gives the impression that the pressure disturbance caused by the finite leading edge did not extend beyond the first full wave of the models, even at maximum boundary layer thickness where the disturbance is expected to be more pronounced. The pressure distribution of the middle waves should thus correspond to that of a wavy wall with infinite chord.

As previously indicated, a rigorous analysis and evaluation of the data has not been conducted under this contract. The remarks in this section should, therefore, be considered as preliminary.

IV. CONCLUDING REMARKS AND RECOMMENDATIONS

The theoretical and experimental investigations performed under this program can be summarized as follows.

1. A new method for solving the flutter equations of low aspect ratio panels is given in section II A.
2. Theoretical predictions of pressure distributions on sinusoidal wavy walls with infinite chord are given in section II B and II C. In section II B, the effects of a turbulent boundary layer is considered. In section II C, the pressure distribution in the transonic range is estimated neglecting boundary layer effects.
3. Experimental investigations concerning the effects of a turbulent boundary layer on the pressure distribution on two dimensional wavy walls are described in section III. In this section a discussion of wind tunnel models, the boundary layer probe and the wind tunnel tests at Ames is given.

The newly developed method for solving the flutter equations of low aspect ratio panels should eliminate most of the computational difficulties experienced with the original program. It is emphasized here that the flutter analysis for low aspect ratio panels given in [1], is not restricted to the pinned edge case so that a treatment of the clamped edge case with in-plane loads is also possible.

Due to various circumstances, only a cursory evaluation of experimental data and a few checks with theoretical predictions have been made so far. This information indicates, however, that the data collected is excellent and that good agreement between theoretical and experimental results can be expected.

It is therefore recommended to continue this program with emphasis on the following objectives.

1. To complete the theoretical investigation of flutter of low aspect ratio panels for the pinned edge case and to extend the analysis to the clamped edge case with in-plane loads.
2. To continue and complete the evaluation and the verification with aerodynamic theories of experimental information gathered on the pressure distribution of the wavy wall models.
3. To collect experimental information on the same wavy wall models at lighter Mach numbers and thicker boundary layers or to start the experimental investigations of the proposed three dimensional wavy wall models.

REFERENCES

[1] Zeydel, E. F. E., "Panel Flutter Aerodynamics," Georgia Institute of Technology, Final Report A-792, September 1965.

[2] Erdelyi, A., et al, Tabels of Integral Transforms, Vol. I, McGraw-Hill, 1954.

[3] Zeydel, E. F. E and A. C. Bruce, "Study of the Pressure Distribution in Low Supersonic Flow with Turbulent Boundary Layer," Quarterly Report No. 2, Project B-208, Georgia Institute of Technology, December 1965.

[4] Zeydel, E. F. E., "Study of the Pressure Distribution on Oscillating Panels in Low Supersonic Flow with Turbulent Boundary Layer," Final Report Project B-208, Georgia Institute of Technology, June 1966.

[5] Garrick, I. E. and S. I. Rubinow, "Flutter and Oscillating Air-Force Calculations for an Airfoil in Two-dimensional Flow, NACA Report 846, 1946.

[6] Hosakawa, I., "Transonic Flow Past a Wavy Wall," Journal of the Physical Society of Japan, Vol. 15, No. 11, pp 2080-2086, November 1960.